Rotationally Invariant Hashing of Median Binary Patterns for Texture Classification

Adel Hafiane[1], Guna Seetharaman[2], Kannappan Palaniappan[1], and Bertrand Zavidovique[3]

[1] Department of Computer Science,
University of Missouri-Columbia, Columbia, MO 65211 USA
[2] Department of Electrical and Computer Engineering,
Air Force Institute of Technology,* Dayton, OH 45433-7765, USA
[3] Institut d'Electronique Fondamentale, Université de Paris-Sud
Bâtiment 220, F-91405 Orsay, France

Abstract. We present a novel image feature descriptor for rotationally invariant 2D texture classification. This extends our previous work on noise-resistant and intensity-shift invariant median binary patterns (MBPs), which use binary pattern vectors based on adaptive median thresholding. In this paper the MBPs are hashed to a binary chain or equivalence class using a circular bit-shift operator. One binary pattern vector (*ie.* smallest in value) from the group is selected to represent the equivalence class. The resolution and rotation invariant MBP (MBP ROT) texture descriptor is the distribution of these representative binary patterns in the image at one or more scales. A special subset of these rotation and scale invariant representative binary patterns termed *uniform* patterns leads to a more compact and robust MBP descriptor (MBP UNIF) that outperforms the rotation invariant uniform local binary patterns (LBP UNIF). We quantitatively compare and demonstrate the advantage of the new MBP texture descriptors for classification using the Brodatz and Outex texture dictionaries.

1 Introduction

Texture analysis and texture-based image classification have been extensively investigated during the last several decades. Image texture plays an important role in many key applications such as content-based image retrieval, medical imaging, remote sensing, surface inspection, visual effects, etc. Several intuitive properties such as coarseness, contrast, regularity, texel or texton shape, color and arrangement are often associated with texture. Although many types of texture features have been proposed [1], there is still no unique mathematical definition of texture that is consistent with perceptual properties of the human visual system. Good

* This work was conducted at the University of Missouri partially supported by NIH award R33-EB00573 and at the University of Paris X1. The conclusions are that of the authors. They do not represent the focus and policies of the Air Force Institute of Technology, USAF or US-DoD.

A. Campilho and M. Kamel (Eds.): ICIAR 2008, LNCS 5112, pp. 619–629, 2008.

texture features that would be reliable for classification tasks need to retain similarity and dissimilarity relationships under various geometric transformations. The importance of enabling existing texture features and discovering new ones that have such geometric invariance properties for constructing texture dictionaries and classification systems has spurred new research in texture analysis, especially supporting rotation, scale, and intensity-shift invariance.

Invariant features can be derived from statistical, structural or spectral texture measures and we describe several representative approaches. The Gray Level Co-occurrence Matrix (GLCM) [2], can be generalized to be rotationally-invariant using all possible angles [3] or polarograms [4]. Models based on Markov Random Fields were extracted to handle rotation by Kashyap and Khotanzad using circular symmetric autoregressive (CSAR) approach [5], and by Mao and Jain using a model-based CSAR [6]. Cohen et al describe rotational textures using Gauss Markov random fields (GMRF) [7]. Rotation-invariant features based on Gabor filters are described by Leung and Peterson [8], Porat and Zeevi used the first and second order statistics of spatially localized features [9], and Haley and Manjunath used a polar analytic form of a two-dimensional (2-D) Gabor wavelet to extract micro-models of texture [10]. Recently, Ojala *et al.* developed a simple but elegant and efficient texture descriptor with gray scale, rotation and scale invariance based on the local binary pattern (LBP) [11]. The LBP is based on the sign of the difference between the central pixel and its neighboring set of pixels. They showed that the invariant LBP combined with local variance descriptors usually provided better texture classification performance in comparison to other well known texture features such as wavelet-based invariant features. Recently Varma and Zisserman [12] use the histogram of local rotationally invariant filter responses to model texture and demonstrated that this is a powerful approach to deal with texture orientation.

In this paper we extend our previously developed median binary pattern (MBP) texture descriptor with noise resistance and gray scale shift invariance [13], to additionally incorporate rotation and scale invariance. The MBP uses the sign of the intensity difference compared to the local median within a neighborhood to describe the local texture microstructure and is more noise resistant than the LBP introduced in [11]. Using fixed size 3×3 neighborhoods at multiple resolutions (an image pyramid) supports the use of fixed size MBPs that are always 9-bits long. However, in the approach of Ojala et al they use circular neighborhoods of different sizes to capture scale invariance which leads to binary strings of different lengths and more complex processing. The length of the LBP in general is one-bit less than the size of the neighborhood since the central pixel is used as the reference, whereas the MBP uses all pixels in the neighborhood and has length equal to the size of the neighborhood. This additional single bit of information turns out to have several important benefits as described later.

Local neighborhood rotations correspond to a shift in the local binary pattern. The group of local rotations is encoded as a sequence of circular bit-shifts which are hashed to a binary chain or equivalence class. This property is further exploited to reduce the number of 9-bit MBP patterns from 512 to 72,

the number of unique equivalence classes, to form the MBP ROT descriptor. Each equivalence class can be identified by a unique class index, for example the binary pattern with the smallest value in that class. The size of each equivalence class varies from one to eight depending on the specific binary pattern. For example, the binary strings 00000000 and 11111111 are singletons, $E_{\#0}$ and $E_{\#255}$ respectively; both 01010101 and 10101010 form class $E_{\#85}$, composed of two elements; whereas, $E_{\#17}$ is an equivalence class with four elements, namely, 00010001, 00100010, 01000100, and 10001000. We use the "#" to emphasize that the indexing is a result of hashing, which is a many to one and irreversible mapping. Thus, #(10101010) = 01010101; and, #(00100010) = #(01000100) = #(10001000) = 00010001. There are 72 distinct classes covering all possible 9-bit MBPs, and the compound hash can be described by a composite function, the first of which maps strings to an equivalence class string followed by a second cardinal mapping to an index. The distribution of the pattern class indices across the image constitutes the proposed texture image descriptor at one scale. It can be represented as a 72×1 vector. Two spatially rotated versions of a highly textured image will each produce nearly equivalent MBP texture descriptors.

The paper is organized as follows: Section 2 describes the original MBP method, Section 3 presents the proposed scheme for rotation and scale invariance, experimental results are given in Section 4, and the conclusions in Section 5.

2 Median Binary Pattern

The Median Binary Pattern (MBP) is determined by mapping from the intensity space to a localized binary pattern by thresholding the pixels against their median value within a neighborhood (typically 3×3). An example is shown in Fig. 1, where the median value is 120. The central pixel is included in this operator, so we obtain 2^9 possible structures. The MBP at pixels (i, j) is,

$$MBP(i,j) = \sum_{i=0}^{L-1} f(a_k) \times 2^k \qquad f(a_k) = \begin{cases} 1 & if \quad a_k \geq Local\_Median \\ 0 & otherwise \end{cases} \tag{1}$$

where L is the size of neighborhood, a_k the pixel intensity value, $MBP \in [0, 511]$ and is a positive integer value. The MBP operator is invariant to monotonic gray-scale changes since the threshold does not depend on a fixed gray level value. The detected pattern is the result of the spatial interactions in the given locality. If there is no contrast within a given neighborhood, it is defined to be a *spot* [11].

The MBP operator is applied at all image pixels, mapping each image pixel to a new 9-bit binary value. The histogram of the MBPs is used to measure the distribution of these patterns over the image and forms the texture descriptor. Thus, the entire image is hashed to a 512×1 vector, i.e., the MBP histogram.

In order to achieve scale invariance, the image is decomposed into several frequency bands using a specific pyramidal subsampling scheme and the MBP histogram is computed for each of these images at each level of the pyramid. Let

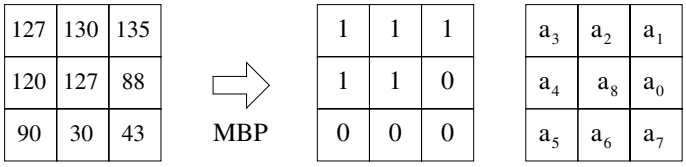

Fig. 1. Example of a median binary pattern with median value of 120, and the pattern $MBP = 100011110_2 \equiv 286$

$\mathcal{I}$ be the original image of size $M \times N$, then, the subsampling process can be described as follows:

$$\begin{aligned} \mathcal{I}_1(i,j) = \mathcal{I}(2i,2j)\ , \mathcal{I}_2(i,j) = \mathcal{I}(2i+1,2j) \\ \mathcal{I}_3(i,j) = \mathcal{I}(2i,2j+1)\ , \mathcal{I}_4(i,j) = \mathcal{I}(2i+1,2j+1) \end{aligned} \tag{2}$$

where $i = 0, 1, 2, \cdots, \lfloor M/2 \rfloor$, $j = 0, 1, 2, \cdots, \lfloor N/2 \rfloor$, and $\mathcal{I}_1, \mathcal{I}_2, \mathcal{I}_3, \mathcal{I}_4$ are a set of four subimages each at half-resolution covering all four-phases. The four-phase images at each resolution helps to capture microstructure relationships between pixels that are not immediate neighbors, for scale independent MBPs.

A histogram of MBPs is computed over the whole image, at each resolution and for each phase, using 512 bins to handle all possible motifs. The histograms for the four-phases are combined into a single histogram at each level (using an order-statistic). The optimal number of resolutions or pyramid levels is application dependent and is empirically chosen as $d = 3$ levels, based on a tradeoff between complexity and performance. Note that increasing the number of levels or frequency subbands does not necessarlity lead to improved texture classification performance. This results in a $(512d)-$dimensional MBP histogram-based feature vector of the pyramid ensemble,

$$H_{MBP} = (H_{MBP}^{(1)}, H_{MBP}^{(2)}, \ldots, H_{MBP}^{(d)}) \tag{3}$$

There are many distance measures that can be used to compare two histograms, and we chose the L_2 norm,

$$\mathcal{D}_{L_2}(H_1, H_2) = \sum_i (H_1(i) - H_2(i))^2 \tag{4}$$

We need to compute the distance between two sets of MBP-histograms. The multi-resolution scale invariant MBP-histogram distance between two textures is computed by finding the minimum across all pairs of resolutions:

$$\mathcal{D} = \min_{d,d'} \left\{ \mathcal{D}_{L2}(H_1^{(d)}, H_2^{(d')}) \right\} \tag{5}$$

3 Rotationally Invariant MBP

The MBP-histogram as described in the previous section is scale invariant but is *not* rotationally invariant. In [13] we demonstrated the effectiveness of the MBP

in categorizing textured images, but also observed that performance degraded when dealing with rotated textures. We extend the MBP-histogram to have rotational invariance by following the approach of Ojala *et al.* [11] with some innovations of our own, primarily by using the central pixel's bit value in the rotation-embedded hashing algorithm.

Local binary patterns are labeled using 9-bit binary numbers based on the MBP operator. When the image is rotated the set of neighbors is geometrically altered, so the binary string pattern is modified and its value changes since the specific order of "1"s and "0"s is different. Fig. 2(a) shows an example of 3×3 pixel intensities, the corresponding MBP is given in Fig. 2(b) where $MBP_1 = 000011111_2$. The string is labeled as: $b_8 b_7 b_6 \cdots b_0$, where b_8 corresponds to the central pixel, and the bits $b_0, b_1, b_2, \cdots, b_7$ correspond to a counter-clockwise ordering starting at the east neighbor (see Fig. 1). Fig. 2(c) shows the same region rotated counter-clockwise, the displacement of values in the neighborhood perimeter in the same as the rotation. Although the median value does not change, the MBP yields a different pattern as shown in Fig. 2(d), $MBP_2 = 001111100_2$. MBP_2 pattern is a circular bit-shift by two of MBP_1 (excluding b_8 the central pixel). Each local rotation produces a shifted binary pattern. In order to make the MBP invariant to this rotation effect, patterns equivalent under shift are considered to belong to the same class, so $MBP_1 \equiv MBP_2$.

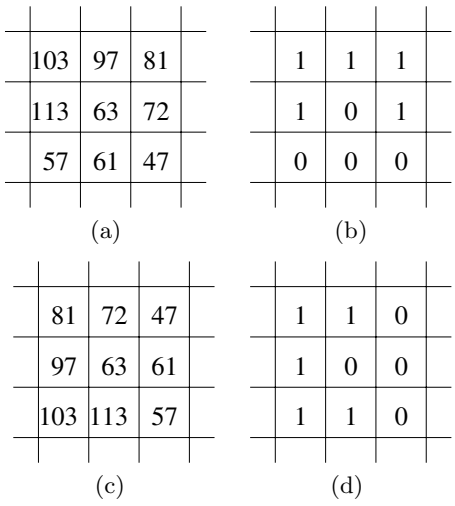

Fig. 2. Example of rotated 3x3 intensities and the corresponding patterns. The instance (b) is assigned the label: 000011111, and the instance (d) is labeled as: 001111100.

3.1 Equivalence Pattern Classes Under Rotation

When an image is subject to a rigid rotation each local neighborhood would undergo nearly the same amount of rotation. The central pixel remains fixed in a relative sense. So b_8, the most significant bit (MSB) remains fixed, while

the lower 8 bits are circularly rotated. For example, the string, $ABCDEFGHI$ transforms to, $ACDEFGHIB$, and is written as:

$$MBP_{ROT}: (\texttt{"ABCDEFGHI"}) := \texttt{"ACDEFGHIB"} \ ; \text{ and,}$$
$$\mathcal{L} \circ \#: \ \texttt{"ABCDEFGHI"} \equiv \texttt{"ACDEFGHIB"}$$

where, MBP_{ROT} is a circular shift function applied to the 8-least significant bits (LSB), and the $\mathcal{L}$ operator is some labeling mechanism. A simple one pass labeling algorithm was developed to identify all equivalence classes over the 256 distinct instances of $b_1, b_2, \cdots, b_8$. Let the index $k, 0 \leq k < 256$ and $k', 0 \leq k' < 256$ be two consecutive members of an equivalence class, then, $k' = 2(k \ \textbf{mod} \ 128) + (k \ \textbf{div} \ 128)$. This search yielded 36 distinct equivalence classes, and, by including the central bit b_8, we arrive at 72 rotation groups, 36 with b_8 off and another 36 with b_8 on. Thus, for all 256 distinct instances of the MBP with $b_8 = 0$, we assign an equivalence class (*i.e.,* a binary chain with 1 to 8 binary patterns), and similarly with $b_8 = 1$.

For example: $MBP_i = 1$ leads to the subsequence $\{1, 2, 4, 8, 16, 32, 64, 128\}$, $MBP_i = 3$ leads to $\{3, 6, 12, 24, 48, 96, 192, 129\}$, as so on. The histogram entries of an MBP at these indexes have a certain mutual impact. Likewise when the image is rotated by 45 degrees the MBP-histogram is modified in a complex manner. However, the trace, defined as the sum of frequency of occurrence of all members within an equivalence group, remains invariant. That is, if one texture is a rotated version of another, then, a secondary histogram, HG derived from the histogram $h[0 \cdots 255]$ of the MBP, as shown below, produces *two* rich sets of 36 features each, invariant to rotations of $45°, 90°, 135°$ etc. The MBP ROT-histogram is,

$$\begin{aligned}
HG(0) &= h(0) \\
HG(1) &= h(1) + h(2) + h(4) + h(8) + ... + h(128) \\
HG(2) &= h(3) + h(6) + h(12) + ...h(192) + h(129) \\
HG(3) &= h(5) + h(10) + h(20) + ... + h(160) + h(65) + h(130) \\
HG(4) &= h(7) + h(14) + \cdots + h(224) + h(193) + h(131) \\
&\vdots \quad \vdots \\
HG(9) &= h(17) + h(34) + h(68) + h(136) \\
HG(10) &= h(19) + h(38) + h(76) + h(152) + h(49) + h(98) + h(196) + h(137) \\
&\vdots \quad \vdots \\
HG(35) &= h(255)
\end{aligned}$$

We propose to establish similarities between two textures using a two step process. The first is to eliminate a large set of improbable matches. This is accomplished by direct comparison of the compound MBP-histograms, HG, using a cross-scale L_2 norm, or weighted Euclidean distance based on *a priori* information about the texture classes. The distance $D_1(A, B)$, is defined as,

$$D_1(A, B) = \min_{d,d'} \Big\{ \sum_{k=0}^{71} \lambda_k (HG_A^{(d)}(k) - HG_B^{(d')}(k))^2 \Big\} \tag{6}$$

It is worth pointing out that the MBPs, 0 do not occur since the threshold is the local median (see Eq. 1, the case of equal intensities generates the all one's binary pattern or 511). Note that the strings will be predominantly mode 4 or 5 suggesting only 5 pixels are above or below the median. The net information content of the histogram H will be limited to a maximum of $\log_2 72$.

3.2 *Uniform Patterns* for Distribution Robustness

Since there are 72 equivalence classes and 3 scales, we have 216 features to determine if two textures are equivalent under rotation and scaling transformations. Notice each group or set gives a different confidence, and each group has independent likelihoods of occurrence. There are some patterns that occur more frequently than others and using only these frequently occurring or *uniform patterns* was observed to improve classification performance of rotated textures [11]. Uniform patterns are defined as those containing at most one transition in the binary string. A uniform pattern satisfies the condition,

$$MBP_{\{ROT,UNIF\}} = MBP_{ROT} \quad if \quad \sum_{k=1}^{7}(a_i - a_{i-1}) \leq 1 \tag{7}$$

Table 1 shows the set of primary uniform patterns satisfying Eq. 7. Obviously the shifted version of the binary pattern is also considered to be a uniform pattern since it belongs to the same equivalence class. However, using only 8 uniform sets drastically reduces the number of bins in the MBP-histograms which may adversely affect texture discrimination. In our case the 9^{th} central-bit helps to increase the discriminative power of the MBP descriptor since it creates additional pattern classes. We separate the 8-bit uniform patterns into two categories with the first one containing sets where $b_8 = 0$, and the second category with $b_8 = 1$. So we have 16 equivalence classes representing the primary uniform MBPs. However due to the median threshold only 10 patterns can occur.

Table 1. Uniform patterns with their natural and binary corresponding values

N	Binary	N	Binary	N	Binary	N	Binary
15	00001111	31	00011111	63	00111111	127	01111111
255	11111111	271	100001111	287	100011111	319	100111111
383	101111111	511	111111111				

4 Experimental Results

Experiments were conducted using two texture dictionaries with rotated textures. The first database is based on the Brodatz album [14], where the images are synthetically rotated. The second set of images is obtained from Outex [15] database with real rotated textures from photos. A supervised classification approach is used to test the performance of the proposed MBP texture descriptors

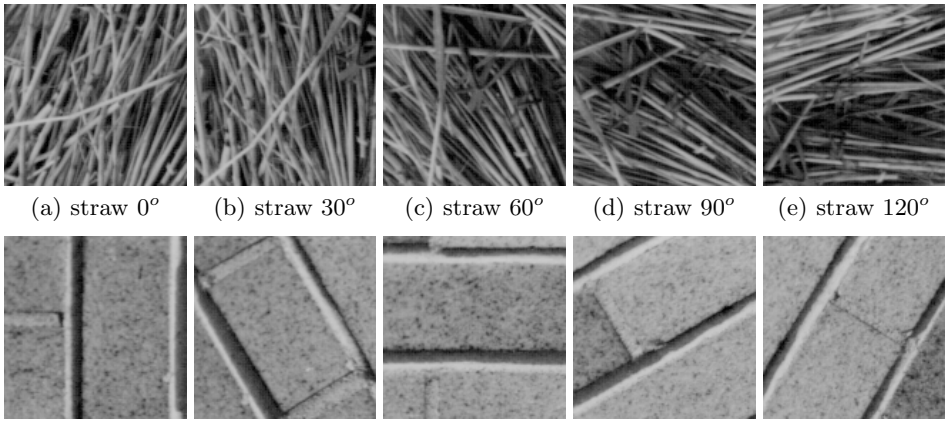

(a) straw 0^o (b) straw 30^o (c) straw 60^o (d) straw 90^o (e) straw 120^o

(f) brick 0^o (g) brick 30^o (h) brick 90^o (i) brick 120^o (j) brick 150^o

Fig. 3. Samples from Brodatz album showing 2 texture classes and 5 synthetic rotations

using the k-Nearest Neighbors classifier (k-NN). The classifier was trained using textures (from the same class) at a few rotation angles and tested on its ability to recognize textures of the same class at any orientation. We use the MBP distance measure in Eq. 5 (or Eq. 6) and $k = 3$ neighbors. Texture samples from each class and different rotations are divided into training and testing groups. The classifier performance for each sample from the test data for each class is averaged to estimate the correct classification accuracy; using $k = 3$ if all retrieved training samples are from the correct class then the score is 100%, two correct matches 66.7% and one correct match 33.3%. We compare the proposed MBP texture descriptor to the LBP (8 neighbor) descriptors in [11]; MBP refers to the original descriptor [13], "MBP ROT" is the MBP rotation (and scale) invariant descriptor and "MBP UNIF" is with rotation invariance and uniform patterns as described, LBP is the original descriptor, "LBP ROT" is with rotation invariance and "LBP UNIF" is with rotation invariance and uniform patterns.

The first experiment used the Brodatz album with 13 classes. Fig. 3 shows samples from two classes with 5 different rotation angles. This example shows the complexity of the problem when the rotation angles are large. Each class contains 16 images (128×128 pixel), each with 6 different rotation angles ($0^o, 30^o, 60^o, 90^o, 120^o, 150^o$) for 96 images per class, and a total of 1248 images in the dictionary. Training textures were rotation angles 0^o and 30^o. The rest of the textures ($60^o, 90^o, 120^o, 150^o$) are used as the test samples for each class. Table 2 shows the results of texture classification. The original MBP and LBP fail to provide good classification accuracy due to their rotation sensitivity (*ie.* brick, raffia, straw, water and wood); some texture classes like grass, sand or weave, have better performance since the texture itself is fairly invariant under geometric transformations. "MBP ROT" and "LBP ROT" show dramatic performance improvements reaching 88.6% and 85.1% respectively, and the best classifier is the "MBP UNIF" at 95.5%.

Table 2. Percentage of correct texture classification for Brodatz dictionary

Class	MBP	MBP ROT	MBP UNIF	LBP	LBP ROT	LBP UNIF
Bark	8.3	**100**	**100**	22.4	93.2	91.2
Brick	0	**98.4**	**98.4**	5.7	95.3	92.7
Bubbles	78.1	98.4	**100**	78.1	89.1	89.1
Grass	47.9	97.4	**100**	28.1	69.3	68.8
Leather	15.1	**100**	**100**	18.2	**100**	**100.0**
Pigskin	16.1	84.4	85.9	20.3	79.2	74.0
Raffia	0	98.4	97.9	0	**100**	98.4
Sand	42.7	**100**	**100**	27.1	96.9	98.4
Straw	4.7	**77.1**	68.2	4.2	75.5	50.5
Water	0	51.6	**100**	0	74.0	77.1
Weave	50.0	**100**	**100**	46.4	98.4	99.0
Wood	0	51.6	**98.4**	0	50.0	94.3
Wool	38.0	**94.3**	92.7	50.0	85.9	87.5
Average	23.2	88.6	**95.5**	23.1	85.1	86.2

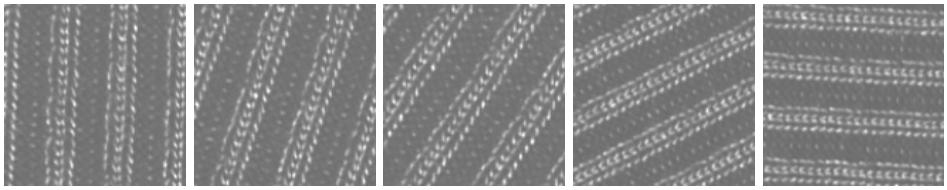

(a) canvas11 0^o (b) canvas11 15^o (c) canvas11 30^o (d) canvas11 60^o (e) canvas11 90^o

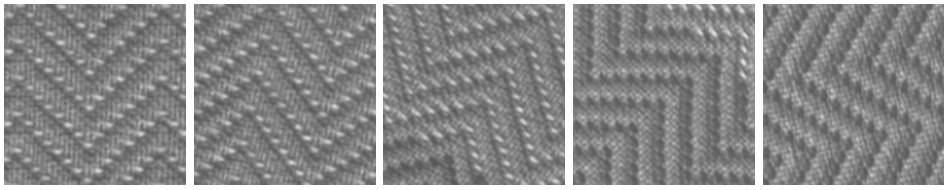

(f) canvas35 0^o (g) canvas35 10^o (h) canvas35 30^o (i) canvas35 45^o (j) canvas35 75^o

Fig. 4. Two textures samples from the Outex database with real rotated textures

The second experiment was performed using the Outex texture database which provides a large collection of textures in many categories under varying conditions of lighting, geometric transformation, resolution, etc. The database we used "Outex_TC_000010" covers oriented textures and contains 24 classes, 20 images (128×128 pixels) per texture class at nine rotation angles ($0^o, 5^o, 10^o, 15^o, 30^o$, $45^o, 60^o, 75^o, 90^o$) for 180 images per class, captured with incandescent CIE illumination at 100 dpi resolution. Fig 4 shows two samples and 5 real orientations. A more rigorous performance evaluation was done by using just *one* texture sample (0^o orientation) for training and the remaining 8 orientations for testing. We evaluate how well the proposed MBP methods can recognize real rotated textures

without any prior training. Table 3 shows that as in the first experiment the original LBP and MBP have weak performance under rotation, and the best classification accuracy of 85% was again achieved by the "MBP UNIF" which improves on the original MBP performance by over 35%. This second more difficult experiment shows the power of the MBP rotation and scale-invariant texture descriptor for texture classification and confirms the surprising result that reducing the size of the texture descriptor by using only the *uniform* binary patterns consistently provides an almost 7% improvement in performance.

Table 3. Percentage of correct texture classification for Outex dictionary

Class	MBP	MBP ROT	MBP UNIF	LBP	LBP ROT	LBP UNIF
Canvas001	60.8	**100**	**100**	75.2	**100**	71.0
Canvas002	70.2	**100**	**100**	51.2	93.1	90.6
Canvas003	87.7	97.5	97.3	98.1	**100**	99.4
Canvas005	36.5	**57.7**	49.2	38.5	52.3	42.5
Canvas006	36.5	60.6	61.9	38.7	**86.2**	58.7
Canvas009	91.9	**100**	**100**	68.7	**100**	**100**
Canvas011	28.1	93.5	**100**	40.6	**100**	**100**
Canvas021	32.9	59.2	**100**	74.6	**100**	**100**
Canvas022	42.9	**100**	**100**	45.2	**100**	98.7
Canvas023	29.4	79.6	78.7	18.3	**94.0**	71.7
Canvas025	21.2	53.7	**79.2**	20.8	76.04	52.7
Canvas026	25.0	55.4	77.9	32.9	**84.3**	78.3
Canvas031	48.7	**98.1**	92.9	43.3	86.9	86.2
Canvas032	34.8	39.6	**84.4**	54.0	42.5	37.1
Canvas033	21.7	**55.0**	46.7	23.7	28.1	25.4
Canvas035	37.5	50.6	**75.0**	40.4	68.3	44.6
Canvas038	41.2	**89.0**	83.1	45.6	81.0	76.7
Canvas039	31.3	59.0	**72.5**	31.9	67.7	58.3
Carpet002	40.0	**91.9**	86.3	39.4	84.8	87.5
Carpet004	93.3	**97.5**	95.6	87.5	79.4	78.7
Carpet005	60.2	**98.1**	96.3	69.4	95.6	95.0
Carpet009	36.5	55.2	69.4	37.5	71.9	**77.7**
Tile005	86.9	98.3	97.1	73.1	98.3	**99.4**
Tile006	86.7	96.9	97.5	90.6	99.4	**99.4**
Average	49.2	78.6	**85.0**	51.6	82.9	76.2

5 Conclusions

We presented a method for rotation and scale invariant texture classification using median binary patterns. The proposed approach handles rotation effects by mapping MBPs to equivalence classes. The histogram of the rotated MBP equivalence classes at multiple scales is used as the texture descriptor. The number of MBP-histogram bins or features is reduced from 512 to 72 using equivalence classes and further reduced to 10, using uniform MBPs which increases

robustness and reduces the computational complexity of the histogram distance calculation. For three subbands, the dimensionality of the MBP texture descriptor is 48. Experiments using 5568 texture samples across two different texture dictionaries (Brodatz and Outex) demonstrated the superior performance of the proposed scale and rotation-invariant MBP descriptor compared to the original MBP. The experiments also quantitatively show that the proposed technique outperforms the equivalent LBP texture features and confirms the advantage of using the uniform patterns. The "MBP UNIF" texture descriptor provides the best combination of rotation, resolution, and gray scale invariance combined with noise resistance.

References

1. Tuceryan, M., Jain, A.K.: Texture analysis. Handbook of pattern recognition & computer vision, 235–276 (1993)
2. Haralick, R.M., Shanmugam, K., Dinstein, I.: Textural features for image classification. IEEE Transactions on Systems, Man, and Cybernetics 3(6), 610–621 (1973)
3. Davis, L.S., Johns, S.A., Aggarwal, J.K.: Texture analysis using generalized co-occurrence matrices. IEEE Transactions on Pattern Analysis and Machine Intelligence 1(3), 251–259 (1979)
4. Davis, L.S.: Polarograms: A new tool for image texture analysis. Pattern Recognition 13(3), 219–223 (1981)
5. Kashyap, R., Khotanzad, A.: A model-based method for rotation invariant texture classification. PAMI 8, 472–481 (1986)
6. Mao, J., Jain, A.K.: Texture classification and segmentation using multiresolution simultaneous autoregressive models. Pattern Recognition 25(2), 173–188 (1992)
7. Cohen, F.S., Fan, Z., Patel, M.A.: Classification of rotated and scaled textured images using gaussian markov random field models. IEEE Transactions on Pattern Analysis and Machine Intelligence 13(2), 192–202 (1991)
8. Leung, M.M., Peterson, A.M.: Scale and rotation invariant texture classification. In: 26th Asilomar Conf Signals, Systems and Comp., pp. 461–465 (1992)
9. Porat, M., Zeevi, Y.Y.: The generalized Gabor scheme of image representation in biological and machine vision. IEEE Trans. PAMI 10(4), 452–468 (1988)
10. Haley, G.M., Manjunath, B.S.: Rotation-invariant texture classification using a complete space-frequency model. IEEE Trans IP 8(2), 255–269 (1999)
11. Ojala, T., Pietikäinen, M., Mäenpää, T.: Multiresolution gray-scale and rotation invariant texture classification with local binary patterns. IEEE Transactions on Pattern Analysis and Machine Intelligence 24(7), 971–987 (2002)
12. Varma, M., Zisserman, A.: A statistical approach to texture classification from single images. International Journal of Computer Vision 62(1-2), 61–81 (2005)
13. Hafiane, A., Seetharaman, G., Zavidovique, B.: Median binary pattern for textures classification. In: ICIAR, pp. 387–398 (2007)
14. Brodatz, P.: Texture: a Photographic Album for Artists and Designers. Dover, New York (1966)
15. Ojala, T., Mäenpää, T., Pietikäinen, M., Viertola, J., Kyllonen, J., Huovinene, S.: Outex - a new framework for empirical evaluation of texture analysis algorithms. In: Proc. 16th Intl. Conf. Pattern Recognition, vol. 1, pp. 706–707 (2002)